Improved device reliability in organic light emitting devices by controlling the etching of indium zinc oxide anode*

Liao Ying-Jie(廖英杰)[a)b)], Lou Yan-Hui(娄艳辉)[a)], Wang Zhao-Kui(王照奎)[a)†], and Liao Liang-Sheng(廖良生)[a)]

[a)] *Jiangsu Key Laboratory for Carbon-Based Functional Materials & Devices, Institute of Functional Nano & Soft Materials (FUNSOM), Soochow University, Suzhou* 215123, *China*

[b)] *College of Electronic Engineering, Jiujiang University, Jiujiang* 332005, *China*

(Received 14 March 2014; revised manuscript received 26 April 2014; published online 17 September 2014)

A controllable etching process for indium zinc oxide (IZO) films was developed by using a weak etchant of oxalic acid with a slow etching ratio. With controllable etching time and temperature, a patterned IZO electrode with smoothed surface morphology and slope edge was achieved. For the practical application in organic light emitting devices (OLEDs), a suppression of the leak current in the current–voltage characteristics of OLEDs was observed. It resulted in a 1.6 times longer half lifetime in the IZO-based OLEDs compared to that using an indium tin oxide (ITO) anode etched by a conventional strong etchant of aqua regia.

Keywords: indium zinc oxide (IZO), organic light emitting device (OLED), leak current, lifetime

PACS: 85.60.Jb, 81.05.Fb, 81.16.Rf **DOI:** 10.1088/1674-1056/23/11/118508

1. Introduction

Organic light-emitting devices (OLEDs) represent a promising technology for large, flexible, light-weight flat-panel displays and solid-state lighting owing to its light weight features, low power consumption, flexibility, and so on.[1–5] For commercial applications of display and lighting, device reliability with longer operational lifetime is one of the main challenging issues. Many intrinsic and extrinsic factors, such as the electrochemical and interfacial degradation, the coverage of particles, and the device encapsulation, affect OLEDs' lifetime.[6–12] In general, transparent conducting oxide (TCO) films like indium tin oxide (ITO) and/or indium zinc oxide (IZO) are widely used as the transparent anode in OLEDs owing to their excellent conductivity and transparency.[13,14] The generation of current in the organic semiconductors relies primarily on direct coating of TCO with conducting organic layers. Several studies have indicated that the lifetime and the performance of OLEDs are strongly affected by the surface morphology of the TCO films and the interface states between the TCO and the organic layers.[15–17] For example, Jonda *et al.* studied the effect of the ITO surface roughness on the degradation of OLEDs with different polymeric thin films.[18] Tak *et al.* reported that the peak to valley roughness of ITO directly affects the reverse leakage current of OLEDs. [19,20] Fukushi *et al.* found that an intrinsic deterioration of the interface between ITO and the organic layer is one of the main factors affecting OLEDs' degradation.[21] In addition, some well-ordered and stable self-assembled monolayers (SAMs) were used to enhance the structure and the morphology of the organic films and improve the charge transfer efficiency between the organic layer and ITO.[22,23]

In general, the TCO films need to be patterned as an electrode with desired emitting shapes before the OLED fabrication. In the conventional patterning methods for the TCO films, the method of dry etching is not generally used due to the difficulty of removing etch products by their poor volatility, which will lower the throughput and increase the cost.[24] Actually, a wet etching method is usually used owing to its advantages of simplification, high throughput, and low cost. However, some issues such as the difficulty of controlling the etching time still exist because the etchants are generally composed of strong acids.[25] In this work, we develop a controllable etching process for IZO patterning by using oxalic acid as an etchant. For comparison, ITO based OLEDs by using the conventional aqua regia as an etchant are also fabricated. In device performance, the IZO-based OLED demonstrates improved half lifetime compared to the ITO-based one.

2. Experiment

The ITO (200 nm) substrates were purchased from GEOMATEC. The IZO films (200 nm) were deposited by sputtering using an IZO target (In_2O_3:ZnO = 90:10) in an Ar atmosphere of 5×10^{-3} Torr with a power of 25 W. The sputtering rate of the IZO films was about 0.7 Å/s. For etching of ITO and IZO, aqua regia and oxalic acid (2.0 wt.%) were used as the etchant, respectively. The etching experiments were performed with the TCO substrates covered with photoresist using the standard lithographic processing. Patterning with 6 μm

*Project supported by the National Natural Science Foundation of China (Grant Nos. 61307036 and 61307037), the Priority Academic Program Development of Jiangsu Higher Education Institutions (PAPD), China, and the University Science Research Project of Jiangsu Province, China (Grant No. 12KJB510028).

†Corresponding author. E-mail: zhaokuiwang@hotmail.com

© 2014 Chinese Physical Society and IOP Publishing Ltd

line widths for the TCO films was carried out for evaluating the electrode shapes. In the etching process, the ITO samples were placed vertically in aqua regia at a temperature of 48 °C, the IZO samples were placed vertically in oxalic acid at varied temperatures for varied etching time to obain an optimized morphology. The end point of etching was confirmed using a multimeter for evaluating the electrical conductivity. The surface roughness of the coated TCO films and the surface morphology of the patterned TCO electrode were evaluated using atomic force microscopy (AFM) and scanning electron microscopy (SEM).

The patterned ITO substrate was thoroughly cleaned and ultraviolet (UV) light was irradiated in a UV ozone chamber under O_2 ambient. Afterward, OLED devices with a typical structure were fabricated by thermal evaporation. N, N′-Diphenyl-N, N′-bis (1-naphthyl)-1, 1′biphenyl -4, 4″ diamine (α-NPD) was used as the hole transport layer and tris(8-hydroxyquinoline) aluminum (Alq_3) was used as both emitting and electron transport layers. LiF was used as a cathode buffer layer. The device structure was ITO (200 nm)/α-NPD (50 nm)/Alq_3 (50 nm)/LiF (1 nm)/Al (70 nm). The OLED devices were completed with encapsulation using a cover glass in a dry nitrogen glove box. The device characteristics were measured using a semiconductor parameter analyzer (HP4155B) and a luminance meter (Topcon). The lifetime of the device, defined as the time degraded to the half luminance value of the initial one, was also evaluated using a hand-made electric circuit system with a computer controlled data logger.

3. Results and discussion

Figure 1 shows the transmission spectra of the reference ITO film (200 nm) and the sputtering IZO film (200 nm). In the short wavelength range (< 620 nm), IZO shows a slightly lower transmission. For example, the transmission of the IZO film is 82.6% at 513 nm (the electroluminescence peak of Alq_3), which is lower than 86.2% of the reference ITO film. However, better transmittance of the sputtering IZO film appears in the longer wavelength range (> 620 nm).

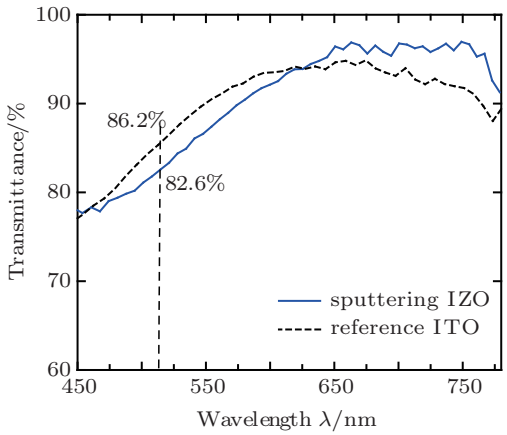


Fig. 1. (color online) The transmittance spectra of the sputtering IZO (200 nm) and the reference ITO (200 nm) films. The dotted line indicates the electroluminescence peak of Alq_3.

Figures 2(a) and 2(b) show the AFM top images of the reference ITO film (200 nm) and the sputtering IZO film (200 nm) with a scanning area of 3 μm ×3 μm, respectively. The root mean square roughness (R_{rms}) of the sputtering IZO film is 2.05 nm, which is larger than that of ITO (1.62 nm). In addition, there are many hillocks on the surface of the IZO film, which have a negative effect on the OLED performance in the conventional viewpoint.

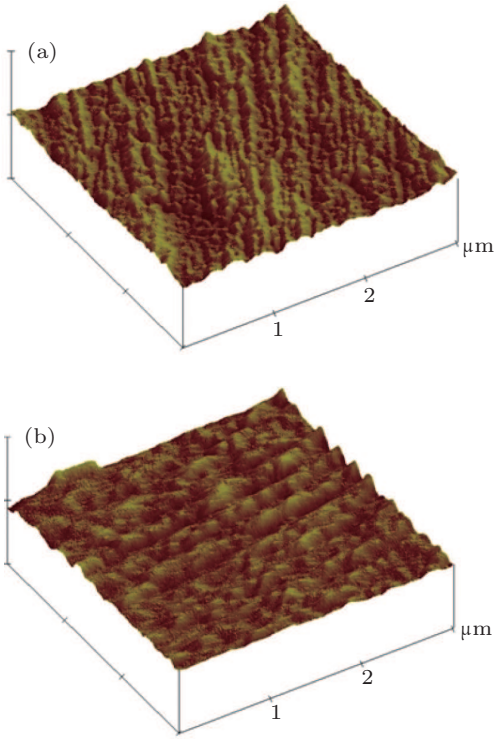


Fig. 2. (color online) AFM top images of (a) the reference ITO film and (b) the sputtering IZO film.

To investigate the effect of etchants on the shapes and the morphologies of the patterned TCO electrodes, patterning with a 6 μm line width for the reference ITO film (200 nm) and the sputtering IZO film (200 nm) is carried out. Figures 3(a)–3(j) show the surface morphologies of the patterned IZO stripes observed by AFM. For comparison, the patterned ITO stripe with aqua regia at a temperature of 48 °C is also shown. Firstly, the dependence of the IZO pattern on the etching time is studied by keeping a fixed temperature of 32 °C. The AFM images of the IZO patterns etched for different times (6–14 min) are shown in Figs. 3(a)–3(e). Obviously, the width of the IZO stripes strongly depends on the etching time. For example, the top width of the IZO stripe remarkably decreases from 6 μm (6 min) to 0.2 μm (14 min). It means that the etching time plays an important role in the final IZO pattern. Therefore, in the practical device fabrication process, careful

control of the etching time for the IZO pattern is necessary. We furthermore investigate the temperature dependence of the IZO pattern by keeping the same etching time (8 min). The corresponding AFM images of the IZO patterns under various temperatures (30–36 °C) are shown in Figs. 3(f)–3(i). There exists no large difference in the top width of the IZO stripes under different temperatures. By changing the etching temperature, only a small effect on the side edge is observed. In all, a better IZO pattern can be obtained by carefully controlling the etching time and the etching temperature using oxalic acid. Figure 3(h) shows the AFM image of the patterned ITO under the optimized condition. It can be seen that the IZO stripe demonstrates a flat top surface with orderly edges. However, there are many rugged regions in the top surface, especially the vertical edge of the ITO stripe. As mentioned above, the rugged surface and edge of the ITO stripe are caused by the rapid and inadequate etching when using aqua regia as the etchant.

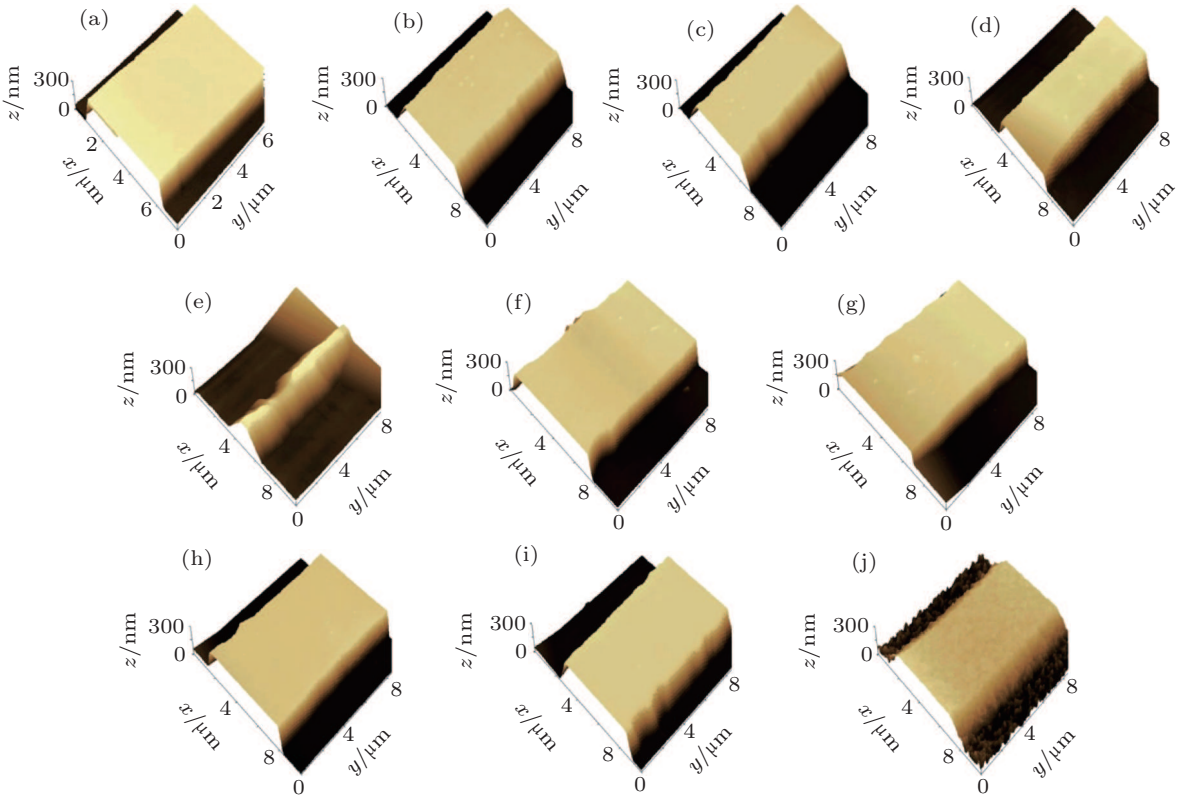


Fig. 3. (color online) AFM images (10 μm × 10 μm) of patterned IZO stripes: (a) 6 min @ 32 °C; (b) 8 min @ 32 °C; (c) 10 min @ 32 °C; (d) 12 min @ 32 °C; (e) 12 min @ 32 °C; (f) 8 min @ 30 °C; (g) 8 min @ 32 °C; (h) 8 min @ 34 °C; (i) 8 min @ 36 °; and patterned ITO stripe: (j) 2 min @ 48 °C.

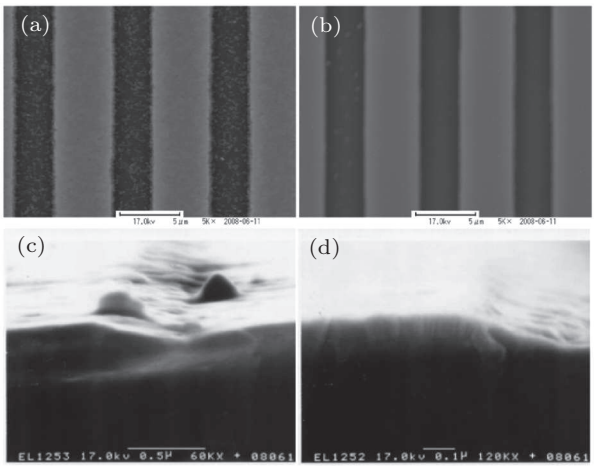


Fig. 4. SEM images of (a) patterned reference ITO film and (b) sputtering IZO film with three stripes. Panels (c) and (d) are the corresponding enlarged SEM images. Every stripe has a width of 6 μm.

Figure 4 shows the SEM images for the ITO film (aqua regia, 2 min @ 48 °C) and the IZO film (oxalic acid, 8 min @ 32 °C) with three stripes (6 μm). Figures 4(c) and 4(d) are the corresponding enlarged SEM images with half a side of one stripe. Although the reference ITO film can be etched with a relative high etching rate by aqua regia, there are a lot of residuals on the glass substrate. Since the rapid etching rate results from the strong acidity of aqua regia, the control of the whole etching, especially the end point of the etching for ITO, is very difficult. Even if prolonging the etching time, the residuals are removed accompanying poor electrode edge and taper angle. Consequently, the residuals originated from the inadequate etching and the poor electrode edge will result in large leak currents in OLEDs. In contrast, the patterned IZO demonstrates a good looking SEM image owing to the con-

trolled etching time by using a weak acid of oxalic acid.

Furthermore, OLED devices using patterned ITO and IZO as the anodes are fabricated to investigate the effects of shapes and morphologies of the patterned electrodes on the device performance. Figures 5(a) and 5(b) show the current density versus voltage (J–V) and the luminance versus current density (L–J) characteristics, respectively. In Fig. 5(a), the turn-on voltage of the sputtering IZO based OLED is 2.4 V, which is slightly lower than that of the reference ITO based OLED (2.8 V). In addition, the IZO based device shows a relatively small leakage compared to the ITO based one. In general, the leakage in the device plays a negative effect on the half lifetime of the OLEDs. From the $L-J$ characteristics shown in Fig. 5(b), no large difference between the ITO- and the IZO-based OLEDs is observed. Both devices demonstrate a maximum luminance of 18000 cd/m^2.

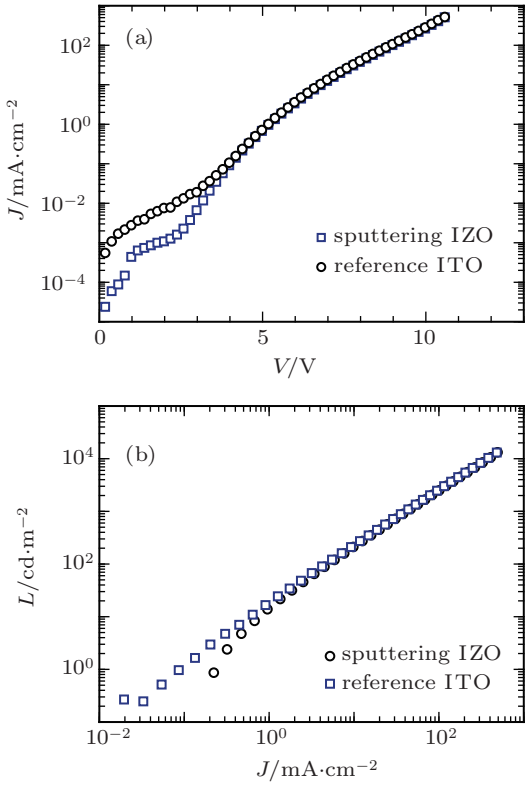


Fig. 5. (color online) OLED performance: (a) current density vs. voltage (J–V) and (b) luminance vs. current density (L–J) characteristics.

Finally, the stabilities of the encapsulated OLEDs by the cover glasses are evaluated under an initial luminance 1000 cd/m^2 as shown in Fig. 6. The IZO-based OLED exhibits a half lifetime of 1830 h, which is 1.6 times longer than that of the ITO based device. Both devices are fabricated and encapsulated at the same round. It suggests that the over quick degradation of the ITO based device is associated with some other factors rather than the device fabricating circumstance and the reaction with atmosphere. Considering the leakage conditions in the J–V characteristics as shown in Fig. 5(a), we ascribe the prolonged half lifetime in the IZO-based OLED to the controllable IZO etching by a weak acid of oxalic acid with improved surface morphology and slope edge for the patterned IZO electrode.

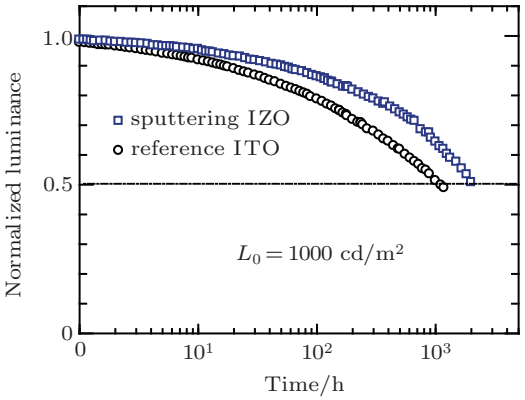


Fig. 6. (color online) Half lifetime measurements for IZO- and ITO-based OLEDs.

4. Conclusion

In summary, we have demonstrated an OLED with a prolonged half lifetime by using an IZO anode, which was etched by a weak etchant of oxalic acid. The OLED based on the ITO anode, which was etched by a strong etchant of aqua regia, was also fabricated for comparison. The surface morphologies and the slope edges of the patterned IZO and ITO films were systematically investigated by SEM and AFM. The experimental results demonstrated that a controllable patterning process for the IZO films could be realized by using a weak etchant of oxalic acid with a low etching rate. As a result, the leakage in the OLED was suppressed and a 1.6 times longer half lifetime was achieved in the IZO based OLED compared to the ITO based one.

References

[1] Forrest S R 2004 *Nature* **428** 911
[2] Zhu X Z, Han Y Y, Liu Y, Lv P, Xu M F, Ruan K Q, Wang Z K, Jie J S and Liao L S 2013 *Org. Electron.* **14** 3348
[3] Qu S, Peng J C and Li H J 2005 *Chin. Phys. Lett.* **22** 719
[4] Peng Y Q, He X Y and Tai X S 2002 *Chin. Phys.* **11** 1076
[5] Wang Z K, Lou Y H, Naka S and Okada H 2011 *AIP Adv.* **1** 032130
[6] Burrows P E, Bulovic V, Forrest S R, Sapochak L S, McCarty D M and Thompson M E 1994 *Appl. Phys. Lett.* **65** 2922
[7] Nan J, Xie Z Y and Dai G R 1998 *Chin. Phys. Lett.* **15** 537
[8] Ma Y G, Tian W J and Shen J C 2000 *Chin. Phys. Lett.* **17** 454
[9] Wang Z K, Naka S and Okada H 2010 *Jpn. J. Appl. Phys.* **49** 01AA02
[10] Popovic Z D and Aziz H 2002 *IEEE J. Select. Topics Quantum Electron.* **8** 362
[11] Aziz H and Popovic Z D 2004 *Chem. Mater.* **16** 4522
[12] Wang Z K, Naka S and Okada H 2009 *Thin Solid Films* **518** 497
[13] Wu C C, Wu C I, Sturm J C and Kahn A 1997 *Appl. Phys. Lett.* **70** 1348
[14] Friend R H, Gymer R W, Holmes A B, Burroughes J H, Marks R N, Taliani C, Bradely D D C, Santos D A D, Bredas J L, Logdlund M and Salaneck W R 1999 *Nature* **397** 121

[15] Nuesch F, Forsythe E W, Le Q T, Gao Y and Rothberg L J 2000 *J. Appl. Phys.* **87** 7973

[16] Hsieh H C, Chang S C and Tsai Y M 2003 *SID 03 Digest* 498

[17] Wang Z K, Lou Y H, Naka S and Okada H 2011 *ACS Appl. Mater. Interfaces* **3** 2496

[18] Jonda C, Mayer A B R, Stolz U, Llschner A and Karbach A 2000 *J. Mater. Sci.* **35** 5645

[19] Tak Y H, Kim K B, Park H G, Lee K H and Lee J R 2002 *Thin Solid Films* **411** 12

[20] Kim K B, Tak Y H, Han Y S, Baik K H, Yoon M H and Lee M H 2003 *Jpn. J. Appl. Phys.* **42** L438

[21] Fukushi Y, Kominami H, Nakanishi Y and Hatanaka Y 2005 *Appl. Sur. Sci.* **244** 537

[22] Choi B, Rhee J and Lee H H 2001 *Appl. Phys. Lett.* **79** 2109

[23] Campbell I H, Kress J D, Martin R L, Smith D L, Barashkov N N and Ferraris J P 1997 *Appl. Phys. Lett.* **71** 3528

[24] Mohir M, Kakinuma H and Sakamoto M 1990 *Jpn. J. Appl. Phys.* **29** 1932

[25] Huang C, Su Y and Wu S 2004 *Mater. Chem. Phys.* **84** 146